TECHNISCHE MECHANIK, Band 22, Heft 4, (2002), 259-270
Manuskripteingang: 05. April 2002

Remarks on Raasch's Hook

H. Schoop, J. Hornig, T. Wenzel

Finite Element's designers have always been seeking for benchmarks to judge the capability and potentiality of a numerical method. Considering shell elements many benchmark tests have been established over the years. The Raasch challenge problem, a clamped curved hook with a tip in-plane shear load, acts as a very interesting benchmark of shell elements. The structure consists of two cylindrical shells with different curvatures. In this paper the problem is also modelled as a curved beam with a rectangular cross-section. The beam model is investigated analytically. Thus an analytical expression for the tip deflection can be obtained. Further on numerical calculations with 4-node-shell elements based on a director theory are carried out and verify the elements applicability.

1 Introduction

One of the biggest difficulties in judging a numerical calculation method is finding a proper example to verify the method. Therefore a benchmark test has to be carried out. In this paper it is done for small displacements. The first basic tests are standard calculations of load cases, which can easily be solved analytically. Another method for verification is analysing one problem with many different numerical process technics. In case of the finite element method one should employ elements based on differing concepts. If more or less all of the methods in use reveal the same results the applicability of a certain element becomes feasible. An arrangement of such examples can be found in literature, e.g. MacNeal and Harder (1985). The example considered is Raasch's Hook problem, for example discussed by Knight (1996) or Kemp,Cho and Lee (1998). The structure is sketched in Figure (1). One end is clamped and the opposite one is free and loaded as described in the foregoing. Geometric and material data are provided in Section (2.1).

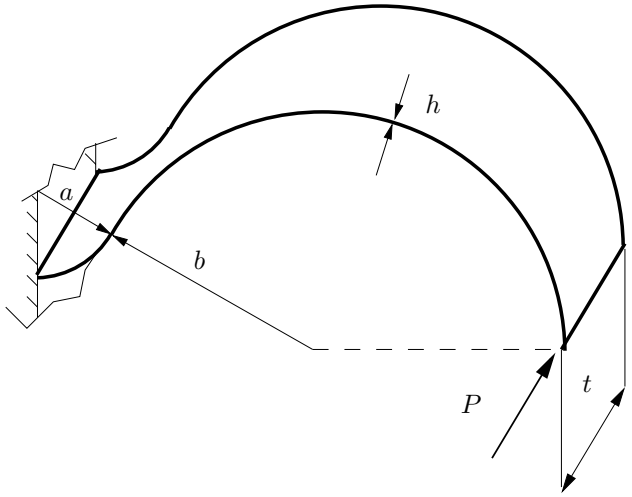

Figure 1: Geometry of Raasch's Hook

2 Preliminary Studies

An analytical solution for the shell model of the hook is not available. Accordingly the analytical solution is based on the theory of curved beams. Firstly, for the sake of simplicity a semicircle arc is discussed. This investigation will reveal the warping effects being outstanding and thus the solution for Raasch's Hook as a curved beam will be derived in Section (3).

2.1 The Semicircle Arc without Warping

The arc is clamped and loaded by a tip load in z-direction. (see Figure (2)).

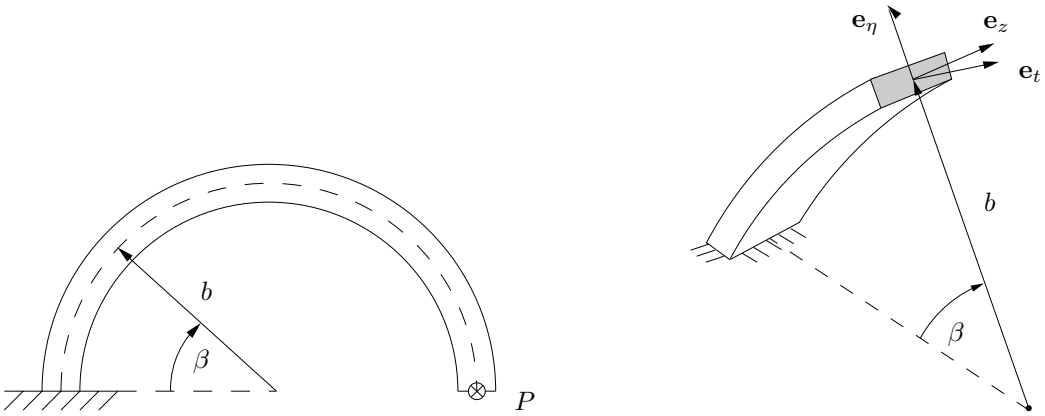

Figure 2: Geometry of the Semicircle Arc

Conditions of Equilibrium Since the arc is borne in a statically determinate manner the balance of forces can be analysed directly. The moment resultant $\mathbf{M}_s = -M_\eta \mathbf{e}_\eta - M_t \mathbf{e}_t + M_z \mathbf{e}_z$ and the stress resultant $\mathbf{F}_s = Q_\eta \mathbf{e}_\eta + N \mathbf{e}_t + Q_z \mathbf{e}_z$ yield as

$$Q_z = P \tag{1}$$
$$M_\eta = -P\, b \sin(\beta) \tag{2}$$
$$M_t = -P\, b\, [1 + \cos(\beta)] \tag{3}$$

All other stress resultants equal zero.

Firstly, the beam shall be investigated with respect to the transverse shear deformation despite any warping effects. At a ratio $\frac{\pi b}{t} = 7.2$, $\frac{\pi b}{h} = 72$, respectively, (see Figures (2) and (3)) it makes sense to utilise the beam model.

The stored complementary energy follows as

$$W^* = \frac{1}{2} \int_0^\pi \left(\frac{M_\eta^2}{EI_{\eta\eta}} + \frac{M_t^2}{GI_t} + \frac{6}{5} \frac{Q_z^2}{GA} \right) b\, d\beta \tag{4}$$

and using Castigliano's first theorem one obtains the tip deflection in the direction of the tip load

$$\frac{\partial W^*}{\partial P} = w(\pi) = P\, \pi \left[\frac{3\, b^3}{2GI_t} + \frac{b^3}{2EI_{\eta\eta}} + \frac{6\, b}{5GA} \right] \tag{5}$$

Material and geometrical data are provided as

$$E = 3300\ psi \qquad \nu = 0.35$$
$$t = 20\ in \qquad h = 2\ in$$

The radius of the bigger arc equals

$$b = 46\ in \quad \text{(see Figures (2) and (3))}$$

and thus the tip deflection comes out to

$$w(\pi) = 7.075\ in$$

Obviously the dominating share of the deflection is the one part due to the torsion. It amounts $99.46\ \%$, whereas the bending has just a very small influence of $0.49\ \%$. The share of the transverse shear is negligible (only 0.05%). Since the influence of the torsion has been outstanding, the ongoing investigation will focus on the torsion problem. The warping effects will be taken into account and the deflection due to transverse shear deformation will be neglected at first, but estimated afterwards.

2.2 The Semicircle Arc with Warping

The theory used to describe the problem in question in a proper manner leans on Wlassow (1964), because it takes into account warping at a curved beam. Although the warping of narrow rectangular cross-sections is usually neglected, since the beam axis remains straight, it will be outlined that the warping share of the total deflection will be approximately 10%, due to the curvature of the beam.

Kinematics of the Curved Beam The coordinates used will be cylindrical ones (β, z) and in direction of the thickness counts η (see Figures (2) and (3)).

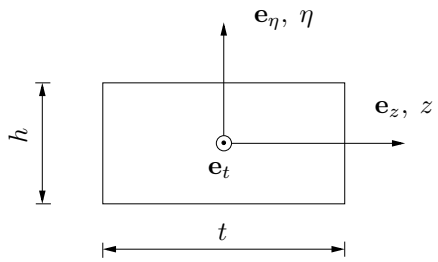

Figure 3: Coordinate System in Cross-section at $\beta = const.$

In order to describe the state of deformation variables are introduced as the following:

$\vartheta\,(\beta)$ angle of torsion

$w\,(\beta)$ deflection in $\mathbf{e}_z$-direction

$\theta\,(\beta)$ slope angle about $\mathbf{e}_\eta$-axis

$f\,(\beta)$ rate of twist

The displacement vector of a material point of the cross-section reads

$$\mathbf{u}\,(\beta,\eta,z) = (z\,\theta + f\,\phi)\,\mathbf{e}_t + \vartheta\,(\eta\,\mathbf{e}_z - z\mathbf{e}_\eta) + w\mathbf{e}_z \tag{6}$$

Each share can be interpreted as:

$(z\,\theta + f\,\phi)\,\mathbf{e}_t$ displacement in tangential direction due to sloping and warping of the cross-section

$\vartheta\,(-z\,\mathbf{e}_\eta)$ displacement in radial direction due to torsion of the cross-section

$\theta\,(\eta\,\mathbf{e}_z)$ displacement in z-direction due to torsion of the cross-section

$w\mathbf{e}_z$ deflection in z-direction

Referring to the straight beam and using the hypothesis of Bernoulli the slope angle and the deflection connect within

$$\theta = -\frac{w'}{b} \tag{7}$$

where $(\ldots)' = \frac{\partial}{\partial\beta}(\ldots)$. As noted in Section (2.1) at this stage of investigation the transverse shear deformation is neglected, thus deflection and slope remain coupled. $\phi(\eta, z)$ denotes the warping function. For the sake of simplicity the warping function of a rectangular cross-section shall be used. This reads $\phi(z, \eta) = z\,\eta$.

The function $f(\beta)$ can be obtained considering the derivative of the rotation vector. The rotation vector consists of two parts in t-, $\eta-$direction, respectively. Its derivative turns out as

$$\frac{\partial}{b\,\partial\beta}\left(\vartheta\mathbf{e}_t+\theta\mathbf{e}_\eta\right)=\frac{\vartheta'+\theta}{b}\mathbf{e}_t+\frac{\theta-\vartheta'}{b}\mathbf{e}_\eta \tag{8}$$

The share in $\mathbf{e}_t$-direction can be identified as the rate of twist $f(\beta)$. From equation (7) it ensues

$$f=\frac{1}{b}\left(\vartheta'-\frac{w'}{b}\right)=\frac{1}{b}\left(\vartheta'+\theta\right) \tag{9}$$

In this case twisting and bending deformation are coupled due to the curvature. Conformingly $f(\beta)$ includes the derivative w'. The term 'rate of twist' refers to Megson (1990).

Constitutive Equations Relating the moment resultants M_η and M_t to the deformation variables w and ϑ and incorporating the kinetic equation according to Wlassow (1964) yields

$$M_\eta = -EI_{\eta\eta}\left(\frac{w''}{b^2}+\frac{\vartheta}{b}\right) \tag{10}$$

$$M_t = -EI_\omega\left(\frac{\vartheta'''}{b^3}-\frac{w'''}{b^4}\right)+GI_t\left(\frac{\vartheta'}{b}-\frac{w'}{b^2}\right) \tag{11}$$

Herein $I_\omega=\int\limits_{(A)}\phi^2dA$ represents the warping constant and EI_ω denotes the warping rigidity (see Timoshenko (1961)). For a narrow rectangular strip that yields $I_\omega=\frac{h^3t^3}{144}$. This share shall here be emphasised, because it is usually neglected.

Determination of the State of Deformation Since the stress resultants have been calculated they are put into equation (10) and equation (11) directly.

$$\left(\frac{w''}{b}+\vartheta\right) = \frac{b}{EI_{\eta\eta}}Pb\sin(\beta) \tag{12}$$

$$\left(\vartheta'''-\frac{w'''}{b}\right)-\frac{GI_t}{EI_\omega}b^2\left(\vartheta'-\frac{w'}{b}\right) = \frac{b^3}{EI_\omega}Pb(1+\cos(\beta)) \tag{13}$$

Equation (13) shows a differential equation for a certain variable $\left(\vartheta-\frac{w}{b}\right)$. Its solution can be obtained as

$$\left(\vartheta-\frac{w}{b}\right)=\frac{C_1}{k}\,e^{k\beta}-\frac{C_2}{k}\,e^{-k\beta}+C_3-\frac{Pb^2}{GI_t}\beta-\frac{1}{1+k^2}\,\frac{b^3}{EI_\omega}\,Pb\,\sin(\beta) \tag{14}$$

where the following abbreviation is used:

$$k^2=\frac{GI_t}{EI_\omega}b^2$$

Supported by equation (14) the angle ϑ can be eliminated from equation (12). Finally a differential equation for the deflection $w(\beta)$ turns out

$$w''+w=\left(\frac{Pb^3}{EI_{\eta\eta}}+\frac{1}{1+k^2}\,\frac{Pb^5}{EI_\omega}\right)\,\sin(\beta)-b\,\frac{C_1}{k}\,e^{k\beta}+b\,\frac{C_2}{k}\,e^{-k\beta}-b\,C_3+\frac{Pb^3}{GI_t}\beta \tag{15}$$

Solving the differential equation (15) the deflection follows as

$$\begin{aligned} w &= -\left(\frac{Pb^3}{EI_{\eta\eta}} + \frac{1}{1+k^2}\,\frac{Pb^5}{EI_\omega}\right)\,\frac{\beta\cos(\beta)}{2} + \frac{Pb^3}{GI_t}\beta + \\ &\quad -\frac{b\,C_1}{k(1+k^2)}\,e^{k\beta} + \frac{b\,C_2}{k(1+k^2)}\,e^{-k\beta} - b\,C_3 + C_4\cos(\beta) + C_5\sin(\beta) \end{aligned} \tag{16}$$

The angle of torsion ϑ leads via equation (14) and equation (16) directly to

$$\begin{aligned} \vartheta &= -\left(\frac{Pb^2}{EI_{\eta\eta}} + \frac{1}{1+k^2}\,\frac{Pb^4}{EI_\omega}\right)\,\frac{\beta\cos(\beta)}{2} + C_1\frac{k}{(1+k^2)}\,e^{k\beta} - C_2\frac{k}{(1+k^2)}\,e^{-k\beta} + \\ &\quad +\frac{C_4}{b}\cos(\beta) + \frac{C_5}{b}\sin(\beta) - \frac{1}{1+k^2}\frac{Pb^4}{EI_\omega}\sin(\beta) \end{aligned} \tag{17}$$

The integration constants C_1 up to C_5 have to be determined by boundary conditions. Where the beam is clamped these are

$$\begin{aligned} w(0) &= 0 \qquad & w'(0) &= 0 \\ \vartheta(0) &= 0 \qquad & \vartheta'(0) &= 0 \end{aligned} \tag{18}$$

At the opposite end boundary conditions are formulated for moments and forces. Because the conditions of equilibrium are satisfied yet, these boundary conditions are satisfied too. Despite the fact that M_η equals zero at the tip the normal stresses σ_{tt} (see equation (19)) in circumferential direction $\mathbf{e}_t$ at the end of the beam have to vanish

$$\sigma_{tt} = \frac{M_\eta}{I_{\eta\eta}}\,z + \phi(\eta,z)\frac{b^2 B(\beta)}{I_\omega} \tag{19}$$

To prevent the violation of this condition the bimoment B (see Wlassow (1964))

$$B = \frac{EI_\omega}{b^2}\left(\vartheta'' - \frac{w''}{b}\right) \tag{20}$$

also has to vanish at the arc's end ($\beta = \pi$). This yields

$$\vartheta'' = \frac{w''}{b} \tag{21}$$

Now the constants C_1 up to C_5 are determined from equations (18) and (21).

$$C_1 = \frac{1}{1+e^{2\,k\,\pi}}\,\frac{2k^2+1}{k^2+1}\,\frac{P\,b^2}{GI_t} \tag{22}$$

$$C_2 = \frac{e^{2\,k\,\pi}}{1+e^{2\,k\,\pi}}\,\frac{2k^2+1}{k^2+1}\,\frac{P\,b^2}{GI_t} \tag{23}$$

$$C_3 = -\frac{1-e^{2\,k\,\pi}}{1+e^{2\,k\,\pi}}\,\frac{2k^2+1}{k\,(k^2+1)}\,\frac{P\,b^2}{GI_t} \tag{24}$$

$$C_4 = -\frac{1-e^{2\,k\,\pi}}{1+e^{2\,k\,\pi}}\,\frac{k\left(2k^2+1\right)}{\left(k^2+1\right)^2}\,\frac{P\,b^3}{GI_t} \tag{25}$$

$$C_5 = Pb^3\,\frac{EI_\omega\left(1+k^2\right)\left[GI_t\left(1+k^2\right) - 2k^2\,EI_{\eta\eta}\right] + EI_{\eta\eta}\,GI_t\left(3+k^2\right)b^2}{2EI_{\eta\eta}\,EI_\omega\,GI_t\,\left(1+k^2\right)^2} \tag{26}$$

Taking into account the warping effects the tip deflection turns out as

$$w(\pi) = 6.437\;in$$

in contrast to $7.075\;in$ without taking into account the warping effects. It becomes quite clear, that these effects are not being negligible, because it makes a difference of approximately 10%. Re-introducing the deflection due

to transverse shear load increases $w(\pi)$. Via

$$w(\pi)_{shear} = \gamma l = 0.003547\ in \tag{27}$$

the total deflection $w(\pi)$ yields $6.441\ in$. The γ in equation (27) equals the constant shear strain due to the constant transverse shear force and l equals the arc length of the semicircle arc.

3 Raasch's Hook as a Curved Beam

Modeling the hook as shown in Figure (4) the beam axis consists of two arcs with the radius a (a-arc) and the radius b (b-arc). The geometrical data are also shown in Figure (4).

$$\alpha_0 = \frac{\pi}{3} \qquad \beta_0 = \frac{\pi}{6} \qquad a = 14\ in \qquad b = 46\ in$$

All other data remain as shown in Section 2.1.

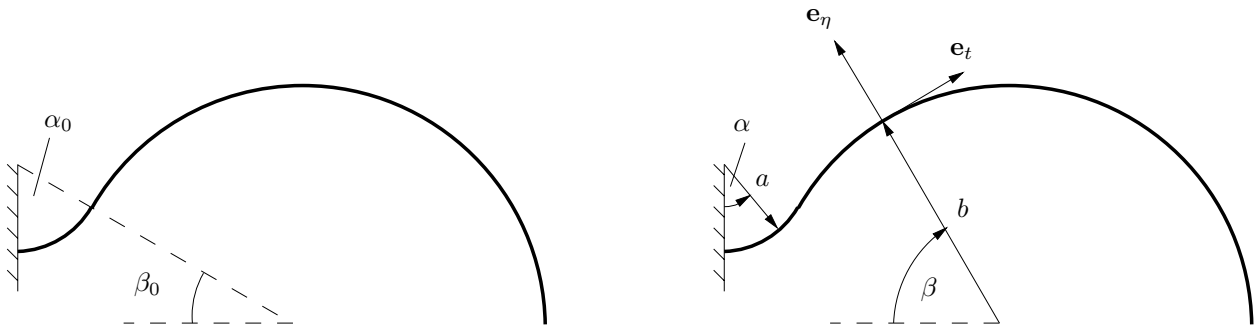

Figure 4: Geometry of Raasch's Hook

Kinematics See Section 2.1. The results outlined in this section shall be taken over.

Constitutive Equations For the a-arc turns out

$$M_\eta(\alpha) = -EI_{\eta\eta}\left(\frac{w^{\cdot\cdot}}{a^2} - \frac{\vartheta}{a}\right) \tag{28}$$

$$M_t(\alpha) = -EI_\omega\left(\frac{\vartheta^{\cdot\cdot\cdot}}{a^3} + \frac{w^{\cdot\cdot\cdot}}{a^4}\right) + GI_t\left(\frac{\vartheta^{\cdot}}{a} + \frac{w^{\cdot}}{a^2}\right) \tag{29}$$

with $w(\alpha)$, $\vartheta(\alpha)$ and $(\ldots)^{\cdot} = \frac{\partial}{\partial\alpha}(\ldots)$ and for the b-arc

$$M_\eta(\beta) = -EI_{\eta\eta}\left(\frac{w''}{b^2} + \frac{\vartheta}{b}\right) \tag{30}$$

$$M_t(\beta) = -EI_\omega\left(\frac{\vartheta'''}{b^3} - \frac{w'''}{b^4}\right) + GI_t\left(\frac{\vartheta'}{b} - \frac{w'}{b^2}\right) \tag{31}$$

The variables and abbreviations $w(\beta)$, $\vartheta(\beta)$, $(\ldots)' = \frac{\partial}{\partial\beta}(\ldots)$ are used, respectively. The changing signs in several terms indicate the change of curvature.

Conditions of Equilibrium Since the problem still remains statically determinate, the stress resultants can directly be calculated. For the a-arc it adds up to

$$M_\eta(\alpha) = P\frac{a+b}{2}\sin(\alpha) - P\left[\frac{\sqrt{3}}{2}a + \left(1+\frac{\sqrt{3}}{2}\right)b\right]\cos(\alpha) \tag{32}$$

$$M_t(\alpha) = Pa - P\left[\frac{\sqrt{3}}{2}a + \left(1+\frac{\sqrt{3}}{2}\right)b\right]\sin(\alpha) - P\frac{a+b}{2}\cos(\alpha) \tag{33}$$

and within the b-arc it adds up to

$$M_\eta(\beta) = -Pb\sin(\beta) \tag{34}$$

$$M_t(\beta) = -Pb\left[1+\cos(\beta)\right] \tag{35}$$

Determination of the State of Deformation The equations (28) up to (31) are solved analogously to the semicircle arc. The deflection within the range $0 \le \alpha \le \alpha_0$ turns out as

$$\begin{aligned} w(\alpha) = & \left(\frac{Pa^2}{EI_{\eta\eta}} + \frac{1}{1+\lambda^2}\,\frac{Pa^4}{EI_\omega}\right)\left(\frac{\sqrt{3}}{2}a + \left(1+\frac{\sqrt{3}}{2}\right)b\right)\frac{\alpha\sin(\alpha)}{2} + \\ & + \left(\frac{Pa^2}{EI_{\eta\eta}} + \frac{1}{1+\lambda^2}\,\frac{Pa^4}{EI_\omega}\right)\left(\frac{a+b}{2}\right)\,\frac{\alpha\cos(\alpha)}{2} + \frac{Pa^3}{GI_t}\alpha + \\ & + \frac{a\,C_1}{\lambda(1+\lambda^2)}\,e^{\lambda\alpha} - \frac{a\,C_2}{\lambda(1+\lambda^2)}\,e^{-\lambda\alpha} - a\,C_3 + C_4\cos(\alpha) + C_5\sin(\alpha) \end{aligned} \tag{36}$$

and within the range $\beta_0 \le \beta \le \pi$ it yields

$$\begin{aligned} w(\beta) = & - \left(\frac{Pb^3}{EI_{\eta\eta}} + \frac{1}{1+k^2}\,\frac{Pb^5}{EI_\omega}\right)\,\frac{\beta\cos(\beta)}{2} + \frac{Pb^3}{GI_t}\beta + \\ & - \frac{b\,C_6}{k(1+k^2)}\,e^{k\beta} + \frac{b\,C_7}{k(1+k^2)}\,e^{-k\beta} - b\,C_8 + C_9\cos(\beta) + C_{10}\sin(\beta) \end{aligned} \tag{37}$$

Herein the abbreviations

$$\lambda^2 = \frac{GI_t}{EI_\omega}a^2 \quad \text{and} \quad k^2 = \frac{GI_t}{EI_\omega}b^2 \tag{38}$$

are used. The angles of torsion can be obtained as

$$\begin{aligned} \vartheta(\alpha) = & -\left(\frac{Pa}{EI_{\eta\eta}} + \frac{1}{1+\lambda^2}\,\frac{Pa^3}{EI_\omega}\right)\left(\frac{\sqrt{3}}{2}a + \left(1+\frac{\sqrt{3}}{2}\right)b\right)\,\frac{\alpha\sin(\alpha)}{2} + \\ & -\left(\frac{Pa}{EI_{\eta\eta}} + \frac{1}{1+\lambda^2}\,\frac{Pa^3}{EI_\omega}\right)\frac{a+b}{2}\,\frac{\alpha\cos(\alpha)}{2} + \\ & + \left(\frac{\sqrt{3}}{2}a + \left(1+\frac{\sqrt{3}}{2}\right)b\right)\frac{1}{1+\lambda^2}\,\frac{Pa^3}{EI_\omega}\cos(\alpha) - \frac{a+b}{2}\frac{1}{1+\lambda^2}\,\frac{Pa^3}{EI_\omega}\sin(\alpha) \\ & + C_1\frac{\lambda}{(1+\lambda^2)}\,e^{\lambda\alpha} - C_2\frac{\lambda}{(1+\lambda^2)}\,e^{-\lambda\alpha} - \frac{C_4}{a}\cos(\alpha) - \frac{C_5}{a}\sin(\alpha) \end{aligned} \tag{39}$$

$$\begin{aligned} \vartheta(\beta) = & -\left(\frac{Pb^2}{EI_{\eta\eta}} + \frac{1}{1+k^2}\,\frac{Pb^4}{EI_\omega}\right)\,\frac{\beta\cos(\beta)}{2} - \frac{1}{1+k^2}\frac{Pb^4}{EI_\omega}sin(\beta) + C_6\frac{k}{(1+k^2)}\,e^{k\beta} + \\ & - C_7\frac{k}{(1+k^2)}\,e^{-k\beta} + \frac{C_9}{b}\cos(\beta) + \frac{C_{10}}{b}\sin(\beta) \end{aligned} \tag{40}$$

respectively.

The constants C_1 up to C_{10} have to be adapted to the boundary conditions and to the conditions at the crossover from the a-arc to the b-arc

$$w(\alpha = 0) = 0 \qquad w(\alpha_0) = w(\beta_0) \tag{41}$$
$$w^{\cdot}(\alpha = 0) = 0 \qquad w^{\cdot}(\alpha_0) = w'(\beta_0) \tag{42}$$
$$\vartheta(\alpha = 0) = 0 \qquad \vartheta(\alpha_0) = \vartheta(\beta_0) \tag{43}$$
$$\vartheta^{\cdot}(\alpha = 0) = 0 \qquad \vartheta^{\cdot}(\alpha_0) = \vartheta'(\beta_0) \tag{44}$$

At the crossover the normal stresses have to stay equal. Consequently the bimoment at the crossover is

$$B(\alpha_0) = B(\beta_0) \quad , \quad \frac{\vartheta^{\cdot\cdot}(\alpha_0)}{a^2} + \frac{w^{\cdot\cdot}(\alpha_0)}{a^3} \quad = \quad \frac{\vartheta''(\beta_0)}{b^2} - \frac{w''(\beta_0)}{b^3} \quad \text{respectively.}$$

At the tip the bimoment must vanish.

$$0 = B(\beta = \pi) \quad , \quad 0 = \vartheta''(\beta = \pi) - \frac{w''(\beta = \pi)}{b} \quad \text{respectively}$$

For the given data the integration constants follow as

$$C_1 = -0.00045424 \qquad C_2 = 0.00322712$$
$$C_3 = 0.01762562 \qquad C_4 = 0.24855690$$
$$C_5 = -0.08721902 \qquad C_6 = 0.0$$
$$C_7 = 6.39958115 \qquad C_8 = 0.02514000$$
$$C_9 = 1.14462473 \qquad C_{10} = -0.58846092$$

The deflection at the tip turns out as

$$w(\beta = \pi) = 4.7457\ in \tag{45}$$

and the angle of torsion yields

$$\vartheta(\beta = \pi) = 0.0263 \tag{46}$$

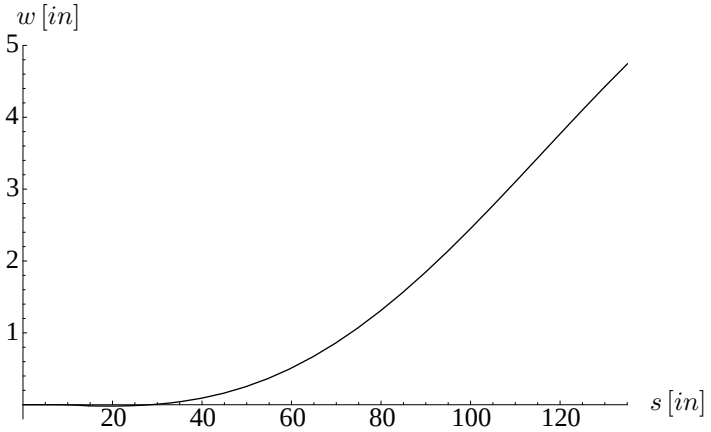

Figure 5: Deflection w over Arclength of the Hook

Incorporating the transverse shear (again as described in equation (27)) the tip displacement is slightly increased. It results in

$$w(\pi) = 4.7561\ in \tag{47}$$

In comparison the answer is approximately 0.2% less stiff than the result neglecting transverse shear deformation.

In order to compare the analytical solution in a proper way with numerical results taken from shell solutions other data are used than cited by Knight (1996) and Kemp, Cho and Lee (1998). Surely the assumptions of the beam theory are much better satisfied if a Hooke material with a Poisson ratio of $\nu = 0.0$ is considered (in contrast to a ratio of $\nu \neq 0.0$). Hence it is interesting to relate the finite element results to the analytical results for a Poisson ratio $\nu = 0.0$. Consequently the numerical analysis with shell elements is carried out for a Poisson ratio $\nu = 0.0$. Thus the element might be "in tune ". The results are compared with the analytical beam solution for the material data $E = 3300\,psi$, $G = 1650\,psi$, respectively.

Afterwards the integration constants turn out as

$$\begin{aligned} C_1 &= -0.0002062 & C_2 &= 0.00237771 \\ C_3 &= 0.01360990 & C_4 &= 0.1913650 \\ C_5 &= -0.0650233 & C_6 &= 0.0 \\ C_7 &= 10.61720 & C_8 &= 0.0180469 \\ C_9 &= 0.827941 & C_{10} &= -0.448799 \end{aligned}$$

Hence the deflection at the free end equals

$$w(\beta = \pi) = 3.5754\,in \tag{48}$$

and the angle of torsion becomes

$$\vartheta(\beta = \pi) = 0.0202 \tag{49}$$

Incorporating the transverse shear (again as outlined in equation (27)) the tip displacement is slightly increased. It adds up to

$$w(\pi) = 3.5831\,in \tag{50}$$

As well as for $\nu = 0.35$ the result for $\nu = 0.0$ is about 0.2% softer than the solution without transverse shear predicts.

4 Numerical Studies with Shell Elements

The calculations are carried out by shell elements that were developed by the authors of this paper. The 4-node elements $Q1$ and $Q1/E4$ (see Wenzel) are both based on an unit director theory with five degrees of freedom per node. The elements do differ in modelling the membrane terms only: While $Q1$ is a pure bilinear displacement element, $Q1/E4$ is improved by the enhanced assumed strain method, which avoids, respectively alleviates in-plane shear locking. The bending problem is solved according to the $\underline{D}$iscrete $\underline{K}$irchhoff $\underline{T}$heory(DKT), which refers to Batoz, Bathe and Ho (1980), Bathe and Ho (1981) or Schoop (1989). These elements neglect the transverse shear deformation.

4.1 Application of Load

The unit Force P applied at the tip of the hook is distributed over all nodes at the edge.

4.2 Numerical Shell Solution and Beam Solution in Comparison

At first the beam solution and the shell solution for $\nu = 0.0$ are compared. Table (1) shows the results of the numerical studies. Additionally the deviations between analytical and numerical solution are given. To judge the convergence the results are also sketched in Figure (6).

mesh	**displacement** $w_{tip}[in]$			**deviation** $[\%]$		
	analy.	$Q1$	$Q1/E4$	analy.	$Q1$	$Q1/E4$
1x9	3.5831	3.664	3.673	-	2.3	2.5
3x17	3.5831	3.582	3.586	-	0.1	0.1
5x34	3.5831	3.569	3.570	-	-0.4	-0.4
10x68	3.5831	3.567	3.567	-	-0.4	-0.4
20x136	3.5831	3.566	3.566	-	-0.5	-0.5

Table 1: Analytical and Numerical Solution in Comparison

Figure (6) shows the displacement $\overline{w}$ of the hook's end, that is normalised by the analytical value $3.5831\ in$. The x-direction indicates the number of elements per arclength.

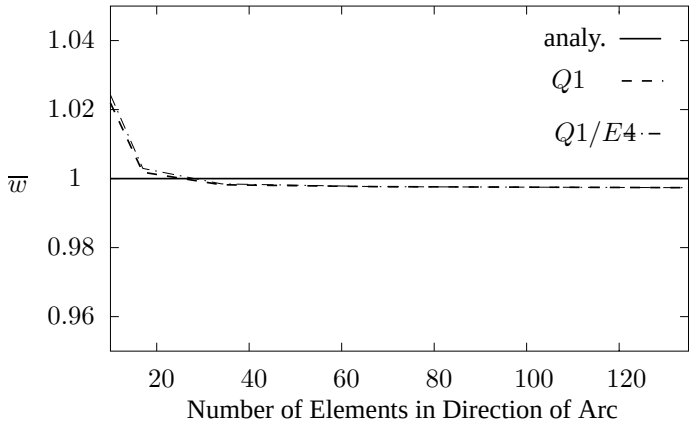

Figure 6: Normalised Displacement $\overline{w}$

Refining the mesh reveals the elements $Q1$ and $Q1/E4$ modelling the structure slightly stiffer than the analytical solution predicts (no transverse shear deformation is taken into account). But this deviation is really small. In case of the 20x136 mesh it amounts only to -0.5%. Both elements are approaching the extrapolated value $3.5661\ in$ (referring to Richardson's method) from above.

4.3 Comparing Different Element Types

As cited by Knight (1996) the calculations are carried out for a Poisson ratio of $\nu = 0.35$. Therefore, the same meshes as presented by Knight (1996) were used. For the sake of comparison the elements $Q1$, $Q1/E4$ and the abaqus elements $S4$ and $S4R5$ were used, too. The results are shown in Table (2). The value $4.7561\ in$ acts as a feasible benchmark, which follows from equation (45). It incorporates the material data $G = 1222.22\ psi$, which belongs to $E = 3300\ psi$,$\nu = 0.35$, respectively.

mesh	**displacement** $w_{tip}\ [in]$						
	$Q1$	$Q1/E4$	$S4$	$S4R5$	$4STG$	$4HYP$	$3DKT$
1x9	4.844	4.853	4.852	28.582	4.4718	5.7061	4.1855
3x17	4.750	4.753	4.867	4.799	4.6381	5.7633	4.6011
5x34	4.727	4.728	4.95	4.829	4.6944	6.8392	4.6776
10x68	4.721	4.721	5.009	4.889	4.7087	10.7424	4.7042
20x136	4.719	4.720	5.033	4.964	4.7121	24.2047	4.6781

Table 2: Different Elements in Comparison

For a better discussion the deviation between the analytical value $4.7561\ in$ and the value calculated by the finest mesh in use is given for all elements in Table (3).

mesh	**deviation** [%]						
	$Q1$	$Q1/E4$	$S4$	$S4R5$	$4STG$	$4HYP$	$3DKT$
20x136	-0.8	-0.8	5.8	4.4	-0.9	>100	-1.6

Table 3: Deviation from Analytical Solution

Both abaqus elements try approaching a significantly higher value than $Q1$ and $Q1/E4$ do. $S4$ and $S4R5$ model the structure softer. The analytical value is quite closer to $Q1$ and $Q1/E4$. According to Hibbitt, Karlsson and Sorensen (2001) the $S4$ is a general purpose shell element, whereas $S4R5$ comprises a quadrilateral small-strain, thin shell element. $S4R5$ also imposes the discrete Kirchhoff constraint. $S4$ holds six degrees of freedom per node, $S4R5$ uses five (as well as $Q1$ and $Q1/E4$ do). Both abaqus elements were integrated fully. All other data and elements refer to Knight (1996). While the element $4STG$ is based on a displacement formulation, $4HYP$ is based on an assumed stress hybrid formulation.

Additionally, the DKT-element $3DKT$ is taken into account. The results w_{tip} are shown in Figure (7) all together.

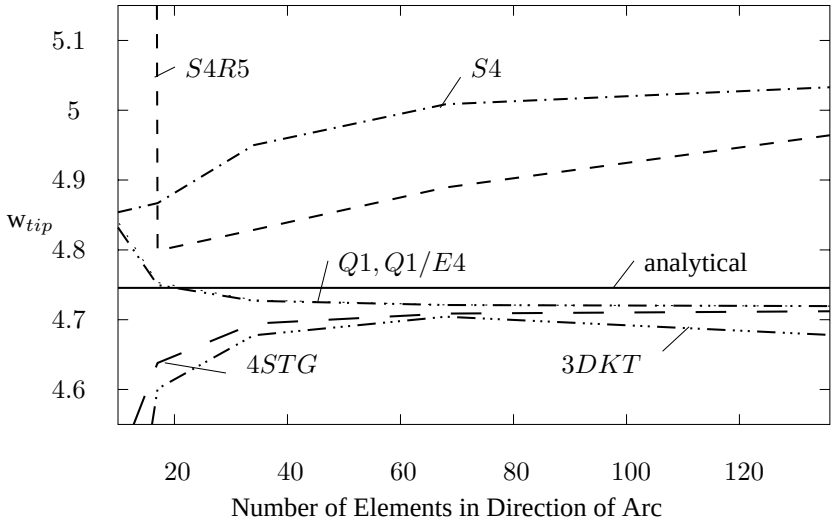

Figure 7: Convergence Study

The first astonishing fact is, that the hybrid element $4HYP$ does not converge, what used to be reported by Knight (1996). Thus its results are not presented inside (Figure 7). Further striking is the convergence of the $3DKT$ element being not quite clear: It firstly approaches convenient values with an increasing number of elements. In contrast to the other elements the deflections predicted by $3DKT$ decrease again. $S4R5$ and $S4$ are both converging from below, but are approaching a softer value than $Q1$ and $Q1/E4$ do. Extrapolated in conformity with Richardson $Q1$ and $Q1/E4$ do converge to $4.7189\ in$ from above. In (Figure 7) the curves of $Q1$ and $Q1/E4$ are virtually congruent. The best correspondence with the elements $Q1$ and $Q1/E4$ at the mesh 20x136 shows the element $4STG$, which misses the extrapolated value about 0.1% only. The $S4$ is about 5.2% and the $S4R5$ is about 6.7% less stiff than the extrapolated value is, although $S4R5$ uses five degrees per node and comprises DKT (as well as the elements $Q1$ and $Q1/E4$ do). In comparison to $4.7561\ in$ $Q1$ and $Q1/E4$ are just slightly stiffer (by about 0.8%). Generally the elements "in tune" $Q1$ and $Q1/E4$ seem to predict a stiffer solution than solutions obtained by continuum elements do. Knight (1996) cites a solution gathered by volume elements for the element $8HYP$ with $4.9352\ in$, whereas abaqus reveals $5.035\ in$ with its element $C3D20R$. In contrast stands the value $4.7561\ in$ based on Wlassow (1964), which indicates a stiffer solution for the deflection in direction of the tip load.

5 Conclusion

The benchmark "Raasch challenge", that is very often used to judge the applicability of finite elements has been investigated and discussed. Therefore it was modelled as a curved beam. After previous studies for the curved semi-circle arc were carried out, Raasch's Hook was calculated analytically according to the theory of Wlassow (1964). The solution obtained outlines that the key role is how to model the torsion problem. The influence of the warping to the deflection is significant and should not be neglected, although the cross-section is a narrow rectangle. Depending upon this fact an analytical solution for a non trivial boundary value problem has been derived, that is based on a reliable theory. Numerical studies have been carried out and a good accordance between analytical solution and solutions obtained by the shell elements $Q1/E4$ and $Q1$ have been observed.

Literature

1. Bathe, K.-J.; Ho, L.W.: A simple and effective shell element for analysis of general shell structures. Comp. & Struc., 13, p. 673-681, (1981)
2. Batoz, J.-L.; Bathe, K.-J.; Ho, L.-W.: A study of three node triangular plate bending elements. Int. J. Numer. Meth. Engng., 15, p. 1771-1812, (1980)
3. Hibbitt, Karlsson & Sorensen Inc.: Abaqus Theory Manual.V. 6.2, (2001)
4. Kemp, B.L.; Cho, C.; Lee, S.W.: A four-node solid shell element formulation with assumed strain. Int. J. Numer. Meth. Engng., 43, p. 909-924, (1998)
5. Knight, N.F. Jr.: The Raasch Challenge for shell elements. AIAA-96-1369-CP, p. 450-460, (1996)
6. MacNeal, R.H.; Harder, R.L.: A proposed standard set of problems to test finite elements accuracy. Finite Elements in Analysis and Design, 1, p. 3-20, (1985)
7. Megson, T.H.G: Aircraft structures for engineering students, Edward Arnold pub., (1990)
8. Schoop,H.: A simple nonlinear flat shell element for large displacement structures. Comp. & Struc., 32, p. 379-385, (1989)
9. Timoshenko, S.P.; Gere, J.M.: Theory of elastic stability. McGraw-Hill, (1961)
10. Wenzel, T.: Finite shell elements with a unit director kinematics. dissertation (in preparation)
11. Wlassow, W.S.: Dünnwandige elastische Stäbe Band 2. VEB Verlag für das Bauwesen Berlin, (1964)

Address: Prof.Dr.-Ing. Heinrich Schoop, Dipl.-Ing. Jörg Hornig, Dipl.-Ing. Thomas Wenzel, Institut für Mechanik - Sekr. MS2, TU Berlin, Einsteinufer 5-7, D-10587 Berlin